Platelet and osteoclast β_3 integrins are critical for bone metastasis

Suzanne J. Bakewell*†, Patrick Nestor†, Srinivasa Prasad‡, Michael H. Tomasson†, Nikki Dowland†, Mukund Mehrotra‡, Robert Scarborough‡, James Kanter‡, Keith Abe‡, David Phillips‡, and Katherine N. Weilbaecher†§

*Department of Physiology and Biophysics, University of Arkansas for Medical Sciences, 4301 West Markham Street, Slot 505, Little Rock, AR 72205; †Departments of Medicine and Pathology, Division of Oncology, Washington University School of Medicine, 660 South Euclid Avenue, Box 8069, St. Louis, MO 63110; and ‡Department of Cardiovascular Biology, Millennium Pharmaceuticals, 256 East Grand Avenue, South San Francisco, CA 94080

Edited by Philip W. Majerus, Washington University School of Medicine, St. Louis, MO, and approved September 12, 2003 (received for review July 12, 2003)

Mice with a targeted deletion of β_3 integrin were used to examine the process by which tumor cells metastasize and destroy bone. Injection of B16 melanoma cells into the left cardiac ventricle resulted in osteolytic bone metastasis in 74% of $\beta_3^{+/+}$ mice by 14 days. In contrast, only 4% of $\beta_3^{-/-}$ mice developed bone lesions. Direct intratibial inoculation of tumor resulted in marrow replacement by tumor in $\beta_3^{-/-}$ mice, but no associated trabecular bone resorption as seen in $\beta_3^{+/+}$ mice. Bone marrow transplantation studies showed that susceptibility to bone metastasis was conferred by a bone marrow-derived cell. To dissect the roles of osteoclast and platelet β_3 integrins in this model of bone metastasis, osteoclast-defective *src*$^{-/-}$ mice were used. Src-null mice were protected from tumor-associated bone destruction but were not protected from tumor cell metastasis to bone. In contrast, a highly specific platelet aggregation inhibitor of activated $\alpha_{IIb}\beta_3$ prevented B16 metastases. These data demonstrate a critical role for platelet $\alpha_{IIb}\beta_3$ in tumor entry into bone and suggest a mechanism by which antiplatelet therapy may be beneficial in preventing the metastasis of solid tumors.

Bone metastases arise by means of a multistep process whereby tumor cells migrate from a primary tumor, disseminate through the arterial system to the bone marrow, and stimulate osteoclast (OC) activation and tumor-associated destruction of cortical and trabecular bone (1–3). Once tumor cells enter the bone marrow cavity, tumor-associated bone destruction (osteolysis) occurs in part through induction of host OC activation. Bisphosphonate OC inhibitors can partially decrease pain, fracture, and cord compression associated with bone metastases; however, ≈50% of bisphosphonate-treated patients can still develop new bone metastases and resultant skeletal complications (4–7). The role of the OC and OC inhibitors in preventing tumor entry into and attachment to bone is unclear.

Venous injection models of "metastasis" have demonstrated that in mice platelet adhesion can play a role in tumor cell lung infiltration (8–15). Gasic *et al*. (8) first demonstrated that lowering the platelet count in mice resulted in decreases in lung invasion after i.v. injection of tumor cell lines. Antibodies directed against platelet antigens involved in tumor adhesion to platelets also decrease lung tumors in mice (9–13) after i.v. tumor cell injection. These observations have been made exclusively in model systems that examine tumor cell growth after passive tumor cell filtration by the pulmonary capillary bed. Furthermore, the molecular mechanisms underlying these phenomena have not been elucidated. Metastasis to other organs and bone could not be evaluated in these venous tumor cell injection systems. We present a report exploring the role of platelets in arterial-mediated metastasis to bone or other visceral organs.

Cell adhesion receptors play roles at multiple stages of metastasis (16–19). We sought to examine the role of host cell β_3-containing integrins in tumor cell metastasis by using mice with a targeted germ-line deletion of the β_3 integrin (β_3) gene. The β_3 integrin subunit heterodimerizes with one of two α-subunits to form $\alpha_{IIb}\beta_3$ ($GPII_bIII_a$) and $\alpha_v\beta_3$ (the vitronectin receptor) (20). $\alpha_{IIb}\beta_3$ is solely expressed by platelets and megakaryocytes and is required for platelet aggregation and hemostasis (21, 22). Mutation in $\alpha_{IIb}\beta_3$ results in the human bleeding disorder Glanzmann's thrombasthenia (23). $\alpha_v\beta_3$ is expressed by multiple cell types including OCs, platelets, megakaryocytes, endothelium, kidney, and placenta (17, 24). $\alpha_v\beta_3$ is expressed progressively by OC precursors as they differentiate, and binding of $\alpha_v\beta_3$ to bone is essential to bone resorption (25–29). β_3 Null ($\beta_3^{-/-}$) animals are born at expected Mendelian frequency, but have dysfunctional platelet aggregation, resulting in bleeding diatheses and a high rate of perinatal mortality (30). Surviving $\beta_3^{-/-}$ pups develop progressive osteosclerosis (with increased bone mass and decreased marrow cavity size) (31). The $\beta_3^{-/-}$ mice have increased numbers of poorly functioning OCs that are multinucleated and tartrate-resistant acid phosphatase (TRAP) positive, but $\beta_3^{-/-}$ OCs are poorly motile with impaired resorptive properties and ruffled border formation (31, 32).

We hypothesized that tumor cells require host β_3 integrins to metastasize to bone and induce bone osteolysis. We injected tumor cells into the arterial circulation of mice to induce bone metastasis (5, 33) and compared the results obtained in WT, β_3 null, and osteopetrotic *src* null animals. We used bone marrow transplantation (BMT) studies to assess the contribution of marrow-derived cells in our model and examined the role of platelet aggregation in this model of bone metastasis by using a specific inhibitor of activated $\alpha_{IIb}\beta_3$ and platelet aggregation.

Methods

Animals. C57B6/129 $\beta_3^{-/-}$ mice were a gift from Steve Teitelbaum (Washington University). C57B6 mice (Harlan Laboratories, Indianapolis) were used for the inhibitor experiments. *Src*$^{-/-}$ mice (C57B6/129) were obtained from The Jackson Laboratory. The Animals Ethics Committee of Washington University approved all experiments.

Cells. B16-F10 mouse melanoma cells (a gift from David Fisher, Dana–Farber Cancer Institute, Boston) were cultured in DMEM with 10% FBS. After 0.1% trypsin/0.2% EDTA treatment, B16 cells were resuspended in PBS before *in vivo* injection. Cell viability was determined by trypan blue exclusion. OCs were formed from bone marrow-derived macrophages in α-MEM containing 10% FCS, 100 ng/ml GST-RANKL (a gift from Paddy Ross, Washington University), and 10 ng/ml macrophage–colony-stimulating factor (R & D Systems) (34). Multinucleated OCs were identified by TRAP staining (Sigma).

Bone Histology and Histomorphometry. Mouse femurs and tibias were fixed in formalin and decalcified in 14% EDTA. Long bones were embedded in paraffin and sliced at equivalent sections coro-

This paper was submitted directly (Track II) to the PNAS office.

Abbreviations: OC, osteoclast; TRAP, tartrate-resistant acid phosphatase; BMT, bone marrow transplantation; LV, left ventricle.

§To whom correspondence should be addressed. E-mail: kweilbae@im.wustl.edu.

nally through the center of the bone. Histological sections were stained with hematoxylin and eosin and stained for TRAP activity. Trabecular bone area was measured according to standard protocol (35) with the Osteomeasure Analysis System (Osteometrics, Decatur, GA).

Bone Metastasis. Mice were anaesthetized following Washington University Animal Committee guidelines. Thirty-gauge needles were used to inject 1×10^5 B16 cells in 100 μl of PBS into the left cardiac ventricle as described (33, 36) with minor modification. To reduce bleeding complications and reduce the incidence of tumor cell extravasation outside the left ventricle (LV), injections were performed with a single needle pass. After the injection, mice were monitored daily for 14 days. All mice were autopsied on day 14 postinjection, and those with extrapleural intrathoracic tumors were excluded from analysis.

Intratibial Injection. Thirty-gauge needles were used to inject 1×10^4 B16 cells or PBS control in 50 μl into the tibia in anaesthetized mice. The knee was flexed, and the needle was inserted into the tibia, boring the needle through the epiphysis and epiphyseal plate for delivery of the cells into the metaphysis. Mice were monitored daily for tumor growth.

BMTs. Mice (aged 6 weeks) were irradiated with 950 rads of γ-radiation. The mice were transplanted with 5×10^6 whole bone marrow cells from $\beta_3^{+/+}$, $\beta_3^{-/-}$, or $\beta_3^{+/+}$ littermates via tail vein injections within 24 h of lethal irradiation. Three weeks after BMT, after normalization of blood counts and bleeding times, mice were LV-injected with B16 cells.

$\alpha_{IIb}\beta_3$ Inhibitor Studies. C57B6 mice were used for the inhibitor studies. ML464 was kindly provided by Millennium Pharmaceuticals, Boston. The active metabolite ML728 of the prodrug ML464 has a serum half-life of 3 h. ML464 or placebo (100 mg/kg) was administered every 12 h via oral gavage for five doses. This dose was selected to obtain maximum platelet inhibition for a period of 12 h during which the concentration of active metabolite ML728 was 37.5 μM at its peak 30 min after oral gavage and 5 μM 8 h after oral gavage of ML464. Thirty minutes after the first oral gavage dose, mice were LV-injected with B16 cells and evaluated for metastases at day 14.

Tumor Cell-Induced Platelet Aggregation. Mouse blood was drawn into 4 units/ml heparin and centrifuged at $200 \times g$ for 20 min to obtain platelet-rich plasma (PRP). PRP was centrifuged at $1,500 \times g$ for 10 min, and platelets were washed in CGS buffer (13 mM trisodium citrate/120 mM sodium chloride/30 mM dextrose, pH 7.0) and resuspended in Hepes-Tyrodes buffer (12 mM sodium bicarbonate/138 mM sodium chloride/5.5 mM glucose/2.9 mM potassium chloride/10 mM Hepes, pH 7.4) containing 1 mM $CaCl_2$ and $MgCl_2$. Washed mouse platelets at 2×10^8/ml were aggregated with 1×10^8/ml B16 cells in the presence or absence of ML728, an active metabolite of ML464. Formation of platelet microaggregates and total aggregates in real time (37) were monitored by laser-light scattering assay in an AG-10 aggregometer (Kowa, Tokyo). Calcein acetoxymethyl ester (Molecular Probes)-labeled washed platelets (2×10^7/ml) were incubated with 1×10^6 B16 cells per ml in the presence or absence of 5 μM ML728.

B16 Adhesion to Spread Platelets. Platelets (2.4×10^7/ml) were allowed to spread in 96-well plates for 1 h at 37°C. Wells were blocked with 2.5% BSA for 30 min at 37°C. B16 cells (8×10^4 per well) were added in the presence or absence of 1 μM fibrinogen and 37.5 μM ML728. Adherent cells were measured with a Cyquant kit assay (Molecular Probes). Flow cytometry of platelet adhesion to B16 cells was performed on B16 cells incubated with unactivated platelets with or without ML728 for 20 min at 37°C. Subsequently, cells were incubated at 37°C for 15 min with anti-mouse $\alpha_{IIb}\beta_3$CD41 antibody (Pharmingen) or isotype control IgG and analyzed by flow cytometry.

Melanoma Cell Adhesion to Fibrinogen. B16 cells were resuspended in serum-free DMEM containing 25 μg/ml soybean trypsin inhibitor, washed, and plated in fibrinogen-coated wells in the presence or absence of ML728 (37.5 μM) or linear RGD peptide (1 mM). Adherent cells were measured with the Cyquant kit.

Results

$\beta_3^{-/-}$ Mice Are Protected from Osteolytic Bone Metastases. To investigate the role of β_3 integrin in development of osteolytic tumor invasion, 6- to 8-week-old $\beta_3^{+/+}$, $\beta_3^{+/-}$, and $\beta_3^{-/-}$ mice were injected with B16F10 murine melanoma cells via the cardiac LV. The overall LV injection procedure-related survival rate in 6-to 12-week-old $\beta_3^{-/-}$ mice was diminished at 59% compared with 93% in $\beta_3^{+/+}$ and 91% in $\beta_3^{+/-}$ mice. Postprocedure thoracotomy was performed on animals that died after LV injection. In each of these cases, the thoracic cavity was filled with blood. The reduced survival of the coagulopathic $\beta_3^{-/-}$ mice after LV injection was therefore attributed to hemorrhage. All of the $\beta_3^{-/-}$ mice that survived the procedure were included in later analyses. The $\beta_3^{+/+}$ mice injected with 1×10^5 B16 cells LV had a mean survival (Kaplan Meier method) of 16 days (data not shown), displaying cachexia (>20% weight loss), labored breathing from chest and lung tumors, and paraplegia from vertebral body tumor invasion and spinal cord compression. Therefore an end-point of 14 days post-LV injection was chosen to evaluate bone metastases.

Fourteen days after B16 LV injection, visible pigmented bone lesions were recorded (Fig. 1*A*), followed by histological confirmation of tumors and associated bone loss in the femurs and tibias (Fig. 1*B*). Histological data showed evidence of bone destruction and OC recruitment in the long bones of $\beta_3^{+/+}$ mice, severe enough in some places to result in disruption of the bone cortex (Fig. 1*B*). In the $\beta_3^{+/+}$ mice, 74% (26/35) developed bone metastases by day 14 (Fig. 1*C*). Heterozygote $\beta_3^{+/-}$ mice developed bone metastases with similar frequency as the $\beta_3^{+/+}$. In contrast, only 1 of 24 of the $\beta_3^{-/-}$ mice injected had histological evidence of bone metastases in the femur and tibia (Fig. 1*C*), whereas the remaining 23 $\beta_3^{-/-}$ mice had no B16 tumors seen in the bone marrow. Visceral metastases were evaluated to confirm that tumor cells successfully entered the arterial system. Eighty one percent of the $\beta_3^{+/+}$ mice had visceral metastases compared with a rate of 63% of the $\beta_3^{-/-}$ mice ($P = 0.20$) (Fig. 1*D*). The sites of visceral metastases (mesentery, adrenal, intestine, kidney, skin, liver, and brain) were not different in the $\beta_3^{+/+}$ and $\beta_3^{-/-}$ mice. We conclude that $\beta_3^{-/-}$ mice are protected from bone metastasis after arterial tumor cell injection.

$\beta_3^{-/-}$ Mice Are Protected from Osteolytic Bone Invasion After Intratibia Tumor Injection. To determine whether the inhibition of the bone metastasis seen in the $\beta_3^{-/-}$ mice reflects a bone microenvironment unable to support tumor cell growth, we inoculated B16 cells or saline directly into the tibial cavity of the $\beta_3^{+/+}$ and $\beta_3^{-/-}$ mice. Fourteen days later, we evaluated tumor cell invasion and measured the induced osteolysis by histomorphometry. Tumor cells proliferated to fill the marrow cavities of both the $\beta_3^{-/-}$ and $\beta_3^{+/+}$ mice (Fig. 2*A*). B16 cells induced significant trabecular bone destruction in the $\beta_3^{+/+}$ tibia compared with saline injection ($P < 0.01$), whereas there was no significant difference in the trabecular bone area between B16- and saline-injected $\beta_3^{-/-}$ tibia (Fig. 2*B*). These data show that B16 melanoma cells cannot induce significant bone destruction in the absence of β_3 integrins in host cells in this model.

Transplantation of $\beta_3^{-/-}$ Bone Marrow Protects WT Mice from Osteolytic Metastases. We hypothesized that the protection we observed in $\beta_3^{-/-}$ mice was caused by dysfunctional OCs or platelets. To eliminate the possibility that β_3 loss in host animal stroma or other cell types was responsible for the protection we observed, we

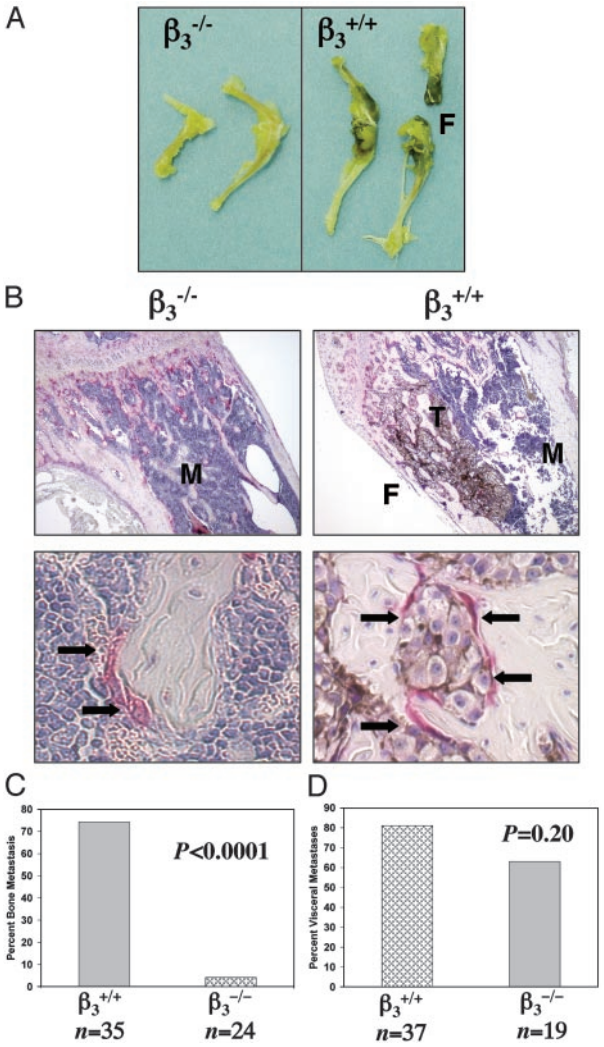

Fig. 1. $\beta_3^{-/-}$ mice are protected from osteolytic bone metastases. (*A*) Visible pigmented B16 melanoma cell bone metastases were seen in $\beta_3^{+/+}$ but not in $\beta_3^{-/-}$ mice, 14 days after B16 tumor cell LV injection. Pathologic fracture (F) developed in $\beta_3^{+/+}$ femur. (*B*) TRAP-stained femur cross section of a B16 LV-injected $\beta_3^{+/+}$ mouse (×4 and ×40 objectives). Pigmented B16 cells (T) are growing throughout the bone marrow (M). Tumor-associated osteolysis induced fracture (F) of bone cortex. Arrows mark TRAP-positive OCs recruited to B16 tumor cells within the bone matrix in $\beta_3^{+/+}$ mice and to trabecular bone/marrow interface in $\beta_3^{-/-}$ mice. No B16 cells were evident in $\beta_3^{-/-}$ femurs in 23/24 mice. (*C*) Percent of mice with bone metastases in femur and tibia 14 days after LV injection of B16 cells for $\beta_3^{+/+}$ compared with $\beta_3^{-/-}$ mice ($P < 0.0001$, Fisher's exact *t* test). (*D*) Percent of mice with pigmented visceral metastases ($P = 0.2$ by Fisher's exact *t* test).

performed BMT by using $\beta_3^{-/-}$ marrow into WT recipients and WT marrow into $\beta_3^{-/-}$ recipients. Bone marrow cells from WT mice were i.v.-injected into lethally irradiated $\beta_3^{-/-}$ mice ($\beta_3^{+/+} > \beta_3^{-/-}$). Recovery of the hematopoietic compartment after BMT was demonstrated by recovery of TRAP+ OCs in the marrow (Fig. 3*A*), recovery of OCs with $\beta_3^{+/+}$ phenotype (Fig. 3*B*), and recovery of platelet aggregation with normalization of bleeding times (Fig. 3*C*). Twenty one days after BMT, 1×10^5 B16 cells were injected via LV. Fourteen days later, the mice were examined for gross and histological evidence of B16 bone invasion. Four of 13 mice (31%) developed B16 bone invasion (Fig. 3*D*). Ten mice (77%) had visceral metastases, confirming successful arterial delivery of the tumor cells (Fig. 3*D*). Thus sensitivity to bone metastases in $\beta_3^{-/-}$ mice was conferred after transplantation of $\beta_3^{+/+}$ marrow.

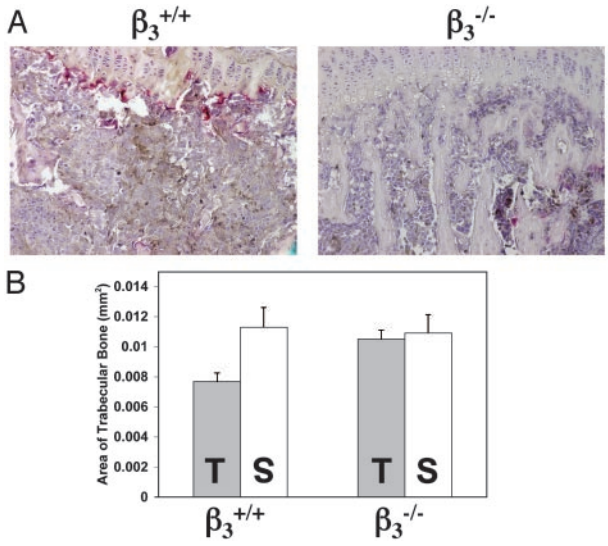

Fig. 2. $\beta 3^{-/-}$ mice are protected from osteolytic bone invasion after direct inoculation of tumor cells into the bone marrow cavity. (*A*) TRAP/hematoxalin staining of $\beta_3^{+/+}$ tibia (*Left*) and $\beta_3^{-/-}$ tibia (*Right*) 14 days after B16 intratibial injection. (*B*) Histomorphometric analysis of trabecular bone area for saline (S) and B16 (T) intratibial-injected tibia (each data point is a compilation of 12 equivalent tibial cross-section measurements taken from four mice with standard error bars). B16 cells induced significant trabecular bone destruction in the $\beta_3^{+/+}$ tibia compared with saline injection ($P < 0.01$ measured by paired *t* test), whereas there was no significant difference seen in $\beta_3^{-/-}$ tibia. $\beta_3^{-/-}$ (T) tibia were protected from tumor-associated trabecular bone loss compared with $\beta_3^{+/+}$ (T) tibia ($P < 0.01$, two-sample *t* test).

One possible explanation for the lower incidence of bone metastases seen in the $\beta_3^{-/-}$ mice reconstituted with WT marrow (31% vs. 74% in $\beta_3^{+/+}$ mice) is that the irradiation used for the BMT inhibited tumor cell growth in bone. To address this, we lethally irradiated 10 $\beta_3^{+/+}$ mice and transplanted $\beta_3^{+/+}$ bone marrow ($\beta_3^{+/+} > \beta_3^{+/+}$) as a control. Forty percent of these $\beta_3^{+/+} > \beta_3^{+/+}$ mice developed bone metastases (a lower rate than 74% in untransplanted $\beta_3^{+/+}$ mice) and 80% had visceral metastases, comparable to the rate seen in $\beta_3^{+/+} > \beta_3^{-/-}$ mice (Fig. 3*D*).

To address the possibility that the protection from bone metastases in the $\beta_3^{-/-}$ mice might also be influenced by abnormal bone microarchitecture, we transplanted $\beta_3^{-/-}$ bone marrow into $\beta_3^{+/+}$ mice ($\beta_3^{-/-} > \beta_3^{+/+}$). Diminished survival rate from the LV tumor cell injection was similar to unirradiated $\beta_3^{-/-}$ mice, with only 7/16 mice (44%) surviving the LV procedure, indicating the presence of $\beta_3^{-/-}$ dysfunctional platelets. Importantly, all seven $\beta_3^{-/-} > \beta_3^{+/+}$ mice were protected from B16 osteolytic bone metastases, whereas four of the mice developed visceral metastases (Fig. 3*D*). These data demonstrate that the susceptibility to bone metastasis is transplantable and are consistent with the hypothesis that the protection we observe in $\beta_3^{-/-}$ mice is conferred by hematopoietic-derived OCs or platelets.

OC-Defective *src*$^{-/-}$ Mutant Mice Develop Bone Lesions Without Tumor-Associated Osteolysis. To determine whether defective OCs in the $\beta_3^{-/-}$ mice are responsible for the protection from bone metastases independent of profoundly abnormal platelet function, we used OC-defective *src*$^{-/-}$ mice. *Src*$^{-/-}$ mice have no reported defects in platelet aggregation, but develop osteopetrosis secondary to defective OC bone resorption (38–41). *Src*$^{-/-}$ mice and *src*$^{+/+}$ littermates were LV-injected with 1×10^5 B16 cells. All of the *src*$^{-/-}$ mice survived the LV injection procedure and had normal bleeding times (1–3 min, $n = 5$), confirming functional platelet aggregation. We cannot rule out that *src*$^{-/-}$ mice have subtle platelet abnormalities. Eighty six percent (6/7 mice) *src*$^{-/-}$ mice and 75% (3/4

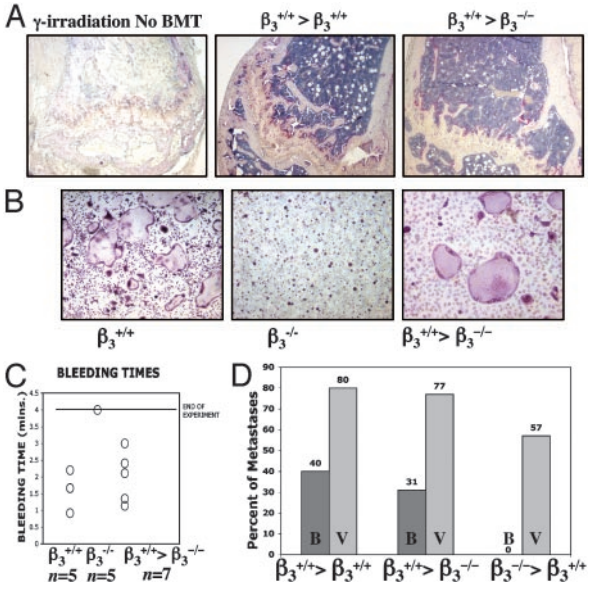

Fig. 3. BMT of $\beta_3^{-/-}$ marrow confers protection from osteolytic metastases. (*A*) (*Left*) TRAP staining of femur 10 days after 950-rad γ-irradiation in untransplanted control mouse demonstrating fatty marrow devoid of red marrow cells and loss of TRAP+ OCs at growth plate. Recovery of TRAP+ OCs is seen at growth plates of femurs 10 days after BMT of $\beta_3^{+/+}$ marrow into $\beta_3^{+/+}$-positive control (*Center*) or into $\beta 3^{-/-}$ mouse (*Right*). (*B*) *In vitro* TRAP staining of cultured OCs results in multinucleated $\beta_3^{+/+}$ OCs with well formed actin rings, compared with $\beta_3^{-/-}$ OCs at day 5. Three weeks after BMT with $\beta_3^{+/+}$ marrow into $\beta_3^{-/-}$ mice restores OC with $\beta_3^{+/+}$ phenotype (*Right*). (*C*) Bleeding times returned to normal range in $\beta_3^{-/-}$ mice 3 weeks after transplantation with $\beta_3^{+/+}$ marrow. (*D*) Percentage of transplanted mice with visible bone metastases (B) and visceral metastases (V) 14 days after LV injection of B16 cells. $\beta_3^{+/+}>\beta_3^{+/+}$ is positive control $\beta_3^{+/+}$ marrow transplanted into $\beta_3^{+/+}$ mouse (n = 10). $\beta_3^{+/+}>\beta_3^{-/-}$ is $\beta_3^{+/+}$ marrow transplanted into $\beta_3^{-/-}$ animals (n = 13), demonstrating that $\beta_3^{+/+}$ marrow can restore ability of B16 to induce bone metastases in $\beta_3^{-/-}$ mice. $\beta_3^{-/-}>\beta_3^{+/+}$ is $\beta_3^{-/-}$ marrow transplanted into $\beta_3^{+/+}$ mice (n = 7), demonstrating that $\beta_3^{-/-}$ bone marrow can protect WT mice from the bone metastases susceptibility as compared with $\beta_3^{+/+}$ mice (P = 0.0004 using the Fisher exact t test).

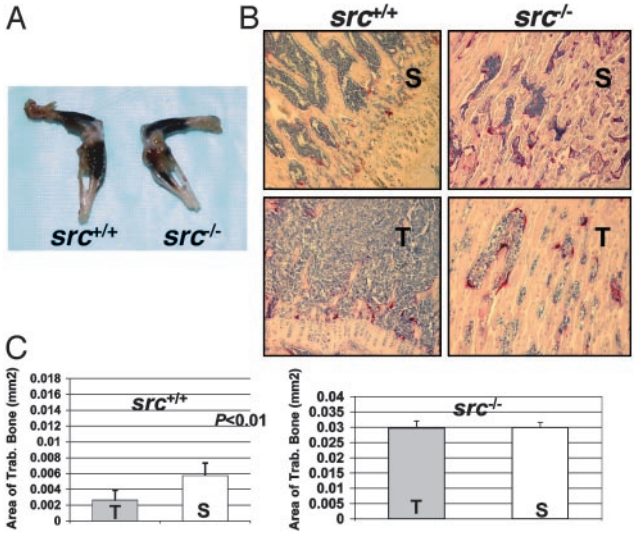

Fig. 4. OC-defective $src^{-/-}$ mutant mice develop bone lesions without tumor-associated bone destruction. (*A*) Visible pigmented B16 melanoma cells bone lesions were seen in $src^{+/+}$ and $src^{-/-}$ mice 14 days after B16 tumor cell LV injection. (*B*) Histology of TRAP-stained tibias from saline LV-injected (S) $src^{+/+}$ and $src^{-/-}$ mice compared with B16 LV-injected (T) mice. B16 cells proliferate to fill available marrow space in both $src^{-/-}$ and $src^{+/+}$ tibia. (*C*) Histomorphometry results show tumor-induced trabecular bone loss in $src^{+/+}$ mice compared with saline-injected mice ($P < 0.01$ by two-sample t test) and no tumor-induced bone loss in B16-injected $src^{-/-}$ mice.

mice) $src^{+/+}$ WT littermates developed widespread visible pigmented bone lesions after LV injection (Fig. 4*A*). Similar rates of visceral metastases were observed in 86% of the $src^{-/-}$ mice and 75% of the $src^{+/+}$ mice. Thus, the OC-defective $src^{-/-}$ mice were not protected from B16 tumor entry into bone, despite the severe osteopetrosis and lack of tumor-induced bone resorption.

The B16 LV-injected into $src^{-/-}$ mice induced little trabecular bone destruction, despite tumor dissemination throughout the marrow cavity (Fig. 4 *B* and *C*). The $src^{+/+}$ WT littermates had B16-associated bone destruction compared with saline-injected controls ($P < 0.01$) (Fig. 4*C*). Because there was little bone destruction in B16 LV-injected $src^{-/-}$ mice and in B16 intratibial-injected $\beta_3^{-/-}$ mice (Fig. 4*C*), we conclude that the B16 cells require functional OCs to induce tumor osteolysis.

These data underscore that the protection from bone metastases seen in the $\beta_3^{-/-}$ mice and reversed by a BMT is not solely explained by lack of proper OC activation and resorption. However, the protection from tumor cells entering the bones of $\beta_3^{-/-}$ mice, not seen in the $src^{-/-}$ mice, is possibly caused by another transplantable hematopoietic cell that is defective in the $\beta_3^{-/-}$mouse, the platelet.

Pharmacologic Inhibition of Platelet $\alpha_{IIb}\beta_3$ Reduces Metastases in $\beta_3^{+/+}$ Mice. ML464 is an orally available member of a spirocyclic series of specific $\alpha_{IIb}\beta_3$ antagonists containing the 2,8-diaza-spiro [4,5]deca-1-one nucleus (M.M., A. Pandey, and R.S., unpublished work). ML464 has a serum half-life of 3 h and is metabolized to form ML728, a competitive inhibitor of murine $\alpha_{IIb}\beta_3$. After oral administration of 100 mg/kg, platelet aggregation, measured by platelet-rich plasma aggregometry, was inhibited within 30 min and remained disrupted for up to 10 h (data not shown). ML728 was used for *in vitro* studies and was found to suppress $\alpha_{IIb}\beta_3$-mediated platelet adhesion to fibrinogen but not $\alpha_2\beta_1$-mediated B16 cell adhesion to collagen, $\alpha_V\beta_3/\alpha_5\beta_1$-mediated adhesion to fibronectin, or $\alpha_6\beta_1$-mediated adhesion to laminin (data not shown). To demonstrate that $\alpha_V\beta_3$ binding of fibrinogen is not inhibited by ML728, we examined adhesion of B16 cells, which express $\alpha_V\beta_3$ but not $\alpha_{IIb}\beta_3$ (42), to a fibrinogen-coated surface in the presence and absence of ML728. Adhesion of B16 cells to fibrinogen was not inhibited by 37.5 μM ML728, whereas 1 mM linear RGD peptide completely blocked adhesion (Fig. 5*A*).

We next sought to investigate the role of platelet β_3 integrin in our metastasis model. ML464 was administered to 40 $\beta_3^{+/+}$ mice by oral gavage at a dose of 100 mg/kg. The mice were treated 30 min before the LV injection of 1×10^5 B16 cells, and then every 12 h for five doses (2.5 days of treatment). Fourteen of 40 (35%) mice died from bleeding complications after the LV injection, indicating effective disruption of $\alpha_{IIb}\beta_3$-mediated platelet aggregation. One of 17 (6%) placebo-treated mice died after the LV injection procedure. The surviving inhibitor-treated mice had significantly less bone metastases (23%) compared with the vehicle-dosed littermates (76%, P = 0.0013) (Fig. 5*B*). A decrease in visceral metastases between placebo and inhibitor-treated mice was also observed (P = 0.0125). Furthermore, we observed that the inhibitor-treated mice that did develop metastases had reduced number and size of visceral metastases compared with the placebo group; however, using this assay we did not measure tumor sizes but instead noted either the presence or absence of metastases.

Previous studies have shown that tumor–platelet interactions can occur directly through $\alpha_{IIb}\beta_3$ or $\alpha_V\beta_3$ (11, 13, 43) and other platelet surface receptors (44). However, we found that B16 adhered to spread platelets and that this interaction was not blocked by ML728 *in vitro* (Fig. 5*C*). To determine whether B16 melanoma cells can stimulate platelet aggregation, we added B16 cells to stirred washed

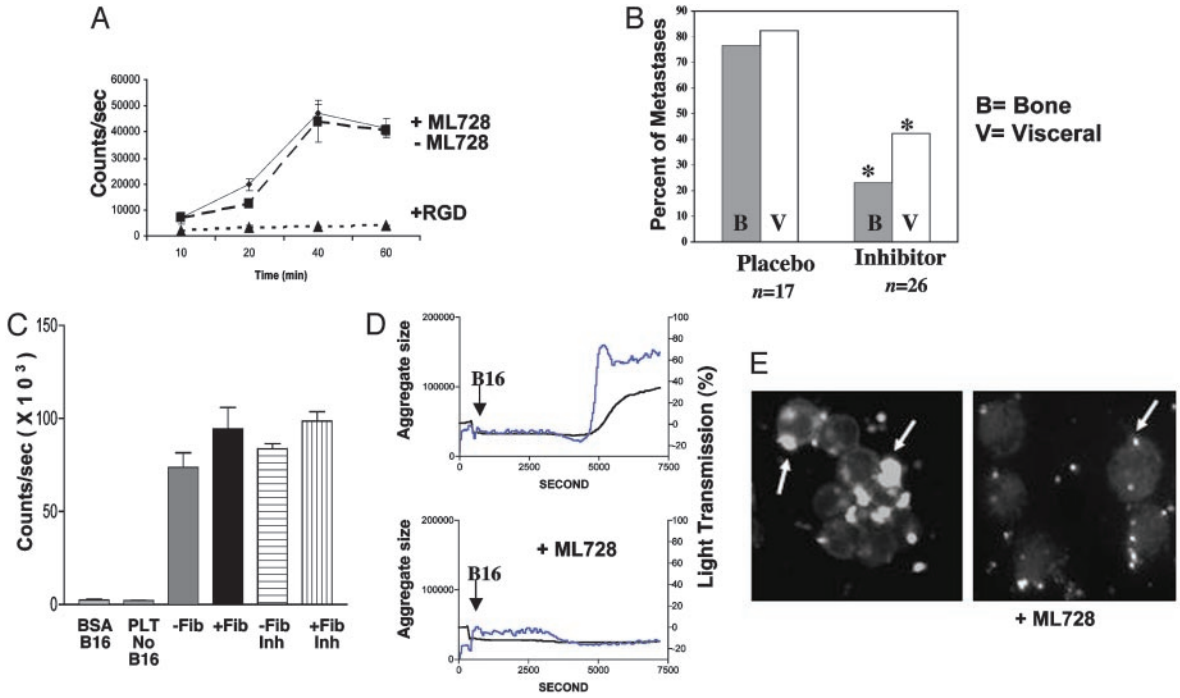

Fig. 5. $\alpha_{IIb}\beta_3$ inhibitor of platelet aggregation reduces metastases in $\beta_3^{+/+}$ mice. ML464 is an oral $\alpha_{IIb}\beta_3$ antagonist. ML728 is the active metabolite of ML464. (*A*) B16 cells spreading on fibrinogen-coated surface (◆) were not inhibited by 37.5 μM ML728 (■) but were completely inhibited by RGD peptide (▲). (*B*) ML464 (inhibitor) was administered to WT ($\beta_3^{+/+}$ mice) 30 min before B16 LV injection and then every 12 h for 2.5 days. Placebo in DMSO carrier was also administered by oral gavage. Mice were evaluated 14 days after B16 injection for bone and visceral metastases. Percentage of mice with bone (B) or visceral (V) metastases or placebo-treated mice (n = 17) and ML464 inhibitor-treated mice (n = 26) is shown. *, Metastases were decreased in inhibitor-treated mice compared with placebo-treated mice (P = 0.0013 for bone and P = 0.0125 for visceral using Fisher's exact t test). (*C*) B16 cells adhered to spread platelets in the presence (+Fib) or absence (−Fib) of fibrinogen, which was not inhibited by ML728 $\alpha_{IIb}\beta_3$ inhibitor (Inh). Platelets alone (PLT no B16) and B16 cells on BSA-coated surface (B16 BSA) served as controls. (*D*) B16 cells added to unactivated platelets induce platelet aggregation as measured in an aggregometer. The arrow represents the addition of B16 cells to platelets. The blue line represents microaggregates, and the black line is total aggregates (micro and large). Addition of 5 μM ML728, an $\alpha_{IIb}\beta_3$ antagonist, to stirred platelets before addition of B16 cells completely inhibited platelet aggregation. (*E*) Calcein-labeled fluorescent mouse platelets adhere to unlabeled B16 tumor cells (arrows) and form aggregates of platelets and tumor cells (*Left*). Addition of 5 μM ML728 inhibited tumor cell and platelet aggregation/clumping but not platelet–tumor cell adhesion (*Right*).

mouse platelets. Platelet microaggregate and large aggregates were formed 6 min after addition of B16 cells (Fig. 5*D*) but not after buffer or COS-7 cells were added (data not shown). B16-stimulated platelet aggregation was inhibited by 5 μM ML728, the active metabolite of the oral $\alpha_{IIb}\beta_3$ antagonist, ML464 (Fig. 5*D Lower*). The IC_{50} for inhibition of B16-stimulated platelet aggregation was 1 μM. Thus, although ML728 did not interfere with tumor adhesion to spread platelets, it did interfere with B16-induced platelet aggregation. Platelet adhesion to B16 cells was also evaluated microscopically when calcein-labeled platelets were incubated with B16 cells. Aggregated platelets bound tumor cells and enhanced crosslinking of tumor cells (Fig. 5*E Left*). Addition of ML728 inhibited platelet aggregation and platelet aggregate mediated crosslinking of B16 cells (Fig. 5*E*). Importantly, however, unaggregated platelets were readily observed on tumor cells in the presence of ML728, indicating that the drug did not inhibit direct platelet binding to tumor cells (Fig. 5*E Right*). Finally, platelet adhesion to B16 cells in the presence and absense of ML728 was analyzed by flow cytometry. Platelets were fluorescently labeled with anti-mouse $\alpha_{IIb}\beta_3$CD41 antibody or isotype control IgG. B16 cells alone were negative for CD41 staining, whereas 10–15% of the B16 cells incubated with platelets were positive for CD41 antibody regardless of the absence or presence of ML728 (data not shown). We conclude that the $\alpha_{IIb}\beta_3$ antagonist, ML464, protected mice from metastasis *in vivo*. However, this $\alpha_{IIb}\beta_3$ antagonist did not disrupt platelet tumor interactions *in vitro*.

Discussion

Tumor metastasis to bone is a multistep process that includes trafficking to the marrow cavity followed by the stimulation of cortical and trabecular bone destruction. We have demonstrated that $\beta_3^{-/-}$ mice are resistant to bone metastasis after intra-arterial injection of tumor cells. Intratibial inoculation of tumor cells resulted in the growth of tumors in the marrow cavity of $\beta_3^{-/-}$ mice without associated bone destruction. Therefore, $\beta_3^{-/-}$ mice supported intramedullary tumor growth after direct intratibial tumor cell injection; however, after arterial LV tumor cell injection, few tumors entered the bone marrow cavity. Taken together, these results suggest that β_3 containing integrins functions in our model both at the level of tumor cell trafficking to bone and tumor-stimulated bone destruction.

The blockade of bone destruction we observed after intratibial injection is consistent with the role of β_3 containing integrins in the development of functional OCs. Bisphosphonate pharmacologic blockade of host OC function has been shown to decrease tumor-associated bone destruction and resultant skeletal complications in patients with metastatic cancer (45). The marked protection from tumor osteolysis we observed in the $src^{-/-}$ and $\beta_3^{-/-}$ mice underscores that host OCs are critical to tumor bone destruction and implicate Src and $\alpha_V\beta_3$ as OC-specific therapeutic antineoplastic targets. In contrast to $src^{-/-}$ mice, $\beta_3^{-/-}$ mice were not only protected from tumor-associated bone destruction but also from migration of tumor cells to bone. These data, in a genetically targeted model of nonfunctioning OCs ($src^{-/-}$ mice), demonstrate that tumor entry into and growth in bone marrow do not depend on functional OCs or osteoclastic resorption and that tumor cells do not directly destroy bone but require src and β_3-expressing host cells. We confirmed that the protection from bone metastases seen in the $\beta_3^{-/-}$ mice was not mediated by microvasculature or other

nonhematopoeitic roles of β_3 integrins by demonstrating that protection from bone metastases could be transferred to recipient mice by BMT. The overall rate of bone metastases compared with visceral metastases was lower after BMT, likely because the irradiated bone microenvironment does not optimally support bone metastases, as has been observed in patients who have undergone radiation therapy (46). Given the nonredundant role of β_3 integrins in platelets, these data suggested to us that platelets were involved in tumor cell trafficking. β_3 Integrin expression serves redundant functions on a variety of cell types residing in the bone marrow in addition to OCs and platelets, so we cannot exclude the possibility that protection was conferred by transplantation of nonhematopoeitic $\alpha_V\beta_3$-expressing cells such as endothelial cells or osteoblasts. However, such nonhematopoeitic transplantation events occur at a low frequency at the 3-week posttransplant time frame (47).

Finally, we found that a highly specific small molecule inhibitor of murine-activated platelet $\alpha_{IIb}\beta_3$ function had a dramatic effect in our model. Our data suggest that the murine $\alpha_{IIb}\beta_3$ antagonist protected mice from bone and visceral metastasis by disrupting platelet–platelet interactions and not platelet–tumor interactions. Alternatively, metastasis in this model may depend on $\alpha_{IIb}\beta_3$ signaling events. Tumor association with platelets has been suggested to play a role in experimental models of venous lung metastases but evaluation of other visceral and bone metastasis is not possible with i.v. tumor models (9–14). In addition, several of these studies could not rule out effects of antiplatelet treatments on tumor cell proliferation and survival because of the cross-reactivity of the agents for tumor cell antigens (9, 10, 12, 13). We have manipulated host cell OCs and platelets in a genetic model and demonstrated that without direct treatment of tumor cells we can decrease metastasis to bone. We have advanced our understanding of the role of platelets in metastasis by using a left cardiac ventricle injection model of bone and visceral metastases using gene-targeted mice and pharmacologic inhibition of platelet aggregation. Importantly, unlike other compounds that have been studied (9, 10, 12, 13), the ML464 $\alpha_{IIb}\beta_3$ inhibitor used here did not disrupt tumor-platelet adhesions *in vitro*. Several possibilities for platelets role in metastasis exist: (*i*) Tumor cell-bound platelets may facilitate adhesion to areas of disrupted vascular endothelium, thereby anchoring tumor cells at distant sites of metastasis. (*ii*) Aggregating platelets on tumor cells could provide paracrine growth and survival factors such as vascular endothelial growth factor and platelet-derived growth factor. (*iii*) Platelet aggregation may cloak tumor antigens, thereby preventing immune-mediated attack. (*iv*) Tumor-associated platelet aggregates or thrombus may mechanically lodge in distant organ microvasculature, allowing tumor entry and metastasis.

Although both $\alpha_{IIb}\beta_3$ inhibitor and $\beta_3^{-/-}$ mice were protected from bone metastases, the $\alpha_{IIb}\beta_3$ inhibitor-treated mice developed fewer visceral metastases compared with the $\beta_3^{-/-}$ mice. Toxicity to B16 cells by ML464 was not observed *in vitro* after incubation with concentrations of drug as high as 55 μM. The difference in the pattern of visceral metastasis between inhibitor-treated and $\beta_3^{-/-}$ mice may therefore be caused by: (*i*) Visceral metastases may depend more on angiogenesis than bone metastases do. $\beta_3^{-/-}$ mice have enhanced tumor-associated angiogenesis with up-regulation of vascular endothelial growth factor receptor expression on tumor-associated blood vessels (48). Increased pathologic angiogenesis in the $\beta_3^{-/-}$ mice could explain the relative lack of protection from visceral metastases seen compared with the $\alpha_{IIb}\beta_3$ inhibitor-treated mice. (*ii*) Nonspecific activities of ML464 affecting metastasis. (*iii*) Strain differences in susceptibility to metastasis may exist between C57B6 strain used for the inhibitor experiments and C57B6/129 strain, which was the background for the $\beta_3^{-/-}$ and WT $\beta_3^{+/+}$ littermates.

Altering platelet and OC β_3 integrin expression impaired tumor cell delivery to bone and tumor-associated bone destruction, respectively. These data argue that in addition to OC-targeted bisphosphonate therapy, small molecule inhibitors of platelet $\alpha_{IIb}\beta_3$ may play an important role in preventing metastasis, the major cause of morbidity and mortality for patients with cancer.

We thank Drs. Steve Teitelbaum and Paddy Ross for their gift of the $\beta_3^{-/-}$ mice and their support and advice during this project; Dr. Stuart Kornfeld for his critical reading of this manuscript; Drs. Kim Trinkhaus and Paula Roberson for help with the biostatistics; and Crystal Idelburg for her expert bone histology slide preparation. S.J.B. is supported by grants from the Barnes-Jewish Foundation and the Edward G. Mallinckrodt, Jr. Foundation. K.N.W. is supported by National Institutes of Health/National Institute on Aging Grant 1K08 AG00852. P.N. is supported by National Institutes of Health Training Grant 5T32HL0708828.

1. Mundy, G. R. (2002) *Nat. Rev. Cancer* **2,** 584–593.
2. Clohisy, D. R. & Ramnaraine, M. L. (1998) *J. Orthop. Res.* **16,** 660–666.
3. Guise, T. A., Yin, J. J., Taylor, S. D., Kumagai, Y., Dallas, M., Boyce, B. F., Yoneda, T. & Mundy, G. R. (1996) *J. Clin. Invest.* **98,** 1544–1549.
4. Lipton, A., Theriault, R. L., Hortobagyi, G. N., Simeone, J., Knight, R. D., Mellars, K., Reitsma, D. J., Heffernan, M. & Seaman, J. J. (2000) *Cancer* **88,** 1082–1090.
5. Yoneda, T., Michigami, T., Yi, B., Williams, P. J., Niewolna, M. & Hiraga, T. (2000) *Cancer* **88,** 2979–2988.
6. Rosen, L. S. (2002) *Semin. Oncol.* **29,** 28–32.
7. Saad, F. (2002) *Semin. Oncol.* **29,** 19–27.
8. Gasic, G. J., Gasic, T. B. & Stewart, C. C. (1968) *Proc. Natl. Acad. Sci. USA* **61,** 46–52.
9. Pearlstein, E., Ambrogio, C. & Karpatkin, S. (1984) *Cancer Res.* **44,** 3884–3887.
10. Karpatkin, S., Pearlstein, E., Ambrogio, C. & Coller, B. S. (1988) *J. Clin. Invest.* **81,** 1012–1019.
11. Felding-Habermann, B., Habermann, R., Saldivar, E. & Ruggeri, Z. M. (1996) *J. Biol. Chem.* **271,** 5892–5900.
12. Francis, J. L. & Amirkhosravi, A. (2002) *Semin. Thromb. Hemostasis* **28,** 29–38.
13. Amirkhosravi, A., Amaya, M. & Siddiqui, F. A. (1999) *Platelets* **10,** 285–292.
14. Felding-Habermann, B., O'Toole, T. E., Smith, J. W., Fransvea, E., Ruggeri, Z. M., Ginsberg, M. H., Hughes, P. E., Pampori, N., Shattil, S. J., Saven, A. & Mueller, B. M. (2001) *Proc. Natl. Acad. Sci. USA* **98,** 1853–1858.
15. Felding-Habermann, B., Fransvea, E., O'Toole, T. E., Manzuk, L., Faha, B. & Hensler, M. (2002) *Clin. Exp. Metastasis* **19,** 427–436.
16. Hynes, R. O. (1992) *Cell* **69,** 11–25.
17. Hood, J. D. & Cheresh, D. A. (2002) *Nat. Rev. Cancer* **2,** 91–100.
18. Teti, A., Migliaccio, S. & Baron, R. (2002) *Calcif. Tissue Int.* **71,** 293–299.
19. Felding-Habermann, B. (2003) *Clin. Exp. Metastasis* **20,** 203–213.
20. Hynes, R. O. (2002) *Cell* **110,** 673–687.
21. Phillips, D. R., Charo, I. F. & Scarborough, R. M. (1991) *Cell* **65,** 359–362.
22. Law, D. A., DeGuzman, F. R., Heiser, P., Ministri-Madrid, K., Killeen, N. & Phillips, D. R. (1999) *Nature* **401,** 808–811.
23. Chen, Y. P., Djaffar, I., Pidard, D., Steiner, B., Cieutat, A. M., Caen, J. P. & Rosa, J. P. (1992) *Proc. Natl. Acad. Sci. USA* **89,** 10169–10173.
24. Brooks, P. C., Clark, R. A. & Cheresh, D. A. (1994) *Science* **264,** 569–571.
25. Horton, M. A., Taylor, M. L., Arnett, T. R. & Helfrich, M. H. (1991) *Exp. Cell Res.* **195,** 368–375.
26. Ross, F. P., Chappel, J., Alvarez, J. I., Sander, D., Butler, W. T., Farach-Carson, M. C., Mintz, K. A., Robey, P. G., Teitelbaum, S. L. & Cheresh, D. A. (1993) *J. Biol. Chem.* **268,** 9901–9907.
27. Engelman, V. W. (1997) *J. Clin. Invest.* **99,** 2284–2292.
28. Rodan, S. B. & Rodan, G. A. (1997) *J. Endocrinol.* **154,** Suppl., S47–S56.
29. Inoue, M., Namba, N., Chappel, J., Teitelbaum, S. L. & Ross, F. P. (1998) *Mol. Endocrinol.* **12,** 1955–1962.
30. Hodivala-Dilke, K. M., McHugh, K. P., Tsakiris, D. A., Rayburn, H., Crowley, D., Ullman-Cullere, M., Ross, F. P., Coller, B. S., Teitelbaum, S. & Hynes, R. O. (1999) *J. Clin. Invest.* **103,** 229–238.
31. McHugh, K. P. (2000) *J. Clin. Invest.* **105,** 433–440.
32. Feng, X., Novack, D. V., Faccio, R., Ory, D. S., Aya, K., Boyer, M. I., McHugh, K. P., Ross, F. P. & Teitelbaum, S. L. (2001) *J. Clin. Invest.* **107,** 1137–1144.
33. Arguello, F., Baggs, R. B. & Frantz, C. N. (1988) *Cancer Res.* **48,** 6876–6881.
34. Weilbaecher, K. N., Motyckova, G., Huber, W. E., Takemoto, C. M., Hemesath, T. J., Xu, Y., Hershey, C. L., Dowland, N. R., Wells, A. G. & Fisher, D. E. (2001) *Mol. Cell* **8,** 749–758.
35. Parfitt, A. M. (1987) *J. Bone Miner. Res.* **2,** 595–610.
36. Kang, Y., Siegel, P. M., Shu, W., Drobnjak, M., Kakonen, S. M., Cordon-Cardo, C., Guise, T. A. & Massague, J. (2003) *Cancer Cell* **3,** 537–549.
37. Tanaka, M., Kawahito, K., Adachi, H., Isawa, H. & Ino, T. (2001) *Artif. Organs* **25,** 719–723.
38. Soriano, P., Montgomery, C., Geske, R. & Bradley, A. (1991) *Cell* **64,** 693–702.
39. Tanaka, S., Amling, M., Neff, L., Peyman, A., Uhlmann, E., Levy, J. B. & Baron, R. (1996) *Nature* **383,** 528–531.
40. Ichinohe, T., Takayama, H., Ezumi, Y., Arai, M., Yamamoto, N., Takahashi, H. & Okuma, M. (1997) *J. Biol. Chem.* **272,** 63–68.
41. Wu, Y., Ozaki, Y., Inoue, K., Satoh, K., Ohmori, T., Yatomi, Y. & Owadab, K. (2000) *Biochim. Biophys. Acta* **1497,** 27–36.
42. Staiano, N., Villani, G. R., Di Martino, E., Squillacioti, C., Vuotto, P. & Di Natale, P. (1995) *Biochem. Mol. Biol. Int.* **35,** 11–19.
43. Silletti, S., Kessler, T., Goldberg, J., Boger, D. L. & Cheresh, D. A. (2001) *Proc. Natl. Acad. Sci. USA* **98,** 119–124.
44. Borsig, L., Wong, R., Hynes, R. O., Varki, N. M. & Varki, A. (2002) *Proc. Natl. Acad. Sci. USA* **99,** 2193–2198.
45. Coleman, R. E. (2002) *Am. J. Clin. Oncol.* **25,** S32–S38.
46. Kaplan, I. D., Valdagni, R., Cox, R. S. & Bagshaw, M. A. (1990) *Int. J. Radiat. Oncol. Biol. Physiol.* **18,** 1019–1025.
47. Lyden, D., Hattori, K., Dias, S., Costa, C., Blaikie, P., Butros, L., Chadburn, A., Heissig, B., Marks, W., Witte, L., *et al.* (2001) *Nat. Med.* **7,** 1194–1201.
48. Reynolds, L. E., Wyder, L., Lively, J. C., Taverna, D., Robinson, S. D., Huang, X., Sheppard, D., Hynes, R. O. & Hodivala-Dilke, K. M. (2002) *Nat. Med.* **8,** 27–34.